

Application of PIXE and PIGE methods for examination of tungsten and rhenium alloys obtained by CVD

V.V.Levenets, A.O.Shchur, O.P.Omelnyk, B.M.Shirokov

National Scientific Center "Kharkiv Institute for Physics and Engineering", National Academy of Sciences of Ukraine,
1 Akademicheskaya St., 61108 Kharkiv, Ukraine,

Received August 28, 2006

The use of nuclear physics methods of ion beam analysis with registration of K-series X-ray and γ -ray from nuclear reactions for determination of tungsten, rhenium and fluorine in binary alloys obtained by chemical vapor deposition has been presented.

Представлено использование ядерно-физических методов на пучках протонов с регистрацией рентгеновского излучения К-серии для определения вольфрама, рения и фтора в двойных сплавах, полученных с помощью газофазного метода, и гамма излучения для определения примеси фтора.

Binary, ternary, and multi-component alloys representing solid solutions on the basis of tungsten are used widely enough as construction materials in high-temperature devices for industrial and household use. A special place among them is occupied by alloys with rhenium concentrations 2–30 wt % [1–3]. However, it is rather difficult to produce such alloys with homogeneous distribution of rhenium in tungsten using the ceramic metal method. Low of diffusion rates of rhenium in tungsten (10^{-14} to 10^{-12} cm²s⁻¹) result in long time of homogeneous alloys formation even at high temperatures (about 2500°C) and the micron sizes of powder [4].

To manufacture binary tungsten-rhenium alloys, a gas-phase method has been used, namely, atomic formation of condensates (chemical vapor deposition-CVD) based on joint reduction of tungsten and rhenium fluorides with hydrogen. The gas-fluoride manufacturing method of such alloys depends on many parameters. The express analytical checking for main elements (tungsten and rhenium) and fluorine impurities in concentrations less than 10^{-3} wt. % is

necessary in technology development and the alloy production and manufacturing of pieces.

It is just the ion beam analysis (IBA) methods of the elemental composition determination using beams of heavy charged particles from electrostatic accelerators that seem to be the most suitable to solve that problem. The particle-induced X-ray emission (PIXE) and particle-induced γ -emission (PIGE) methods are the most versatile and simple of those from the standpoint of sample handling, measurement realization and processing and interpretation of obtained analytical data. These analytical technologies are based on registration of characteristic X-ray emission of atoms and the instantaneous γ -emission of the nuclei caused by interaction of protons with energy up to some MeV with substance. Both methods use the same spectrometric equipment and similar techniques of analytical spectra processing and data obtaining on the quantitative composition of samples being studied. To solve some problems, it is possible to optimize the measurement conditions in

such a manner that both methods may be used jointly and simultaneously.

The purpose of this work is to develop an analysis method of tungsten-rhenium alloys for the content of main components using characteristic X-ray emission of K-series, and also fluorine in concentration 10^{-4} – 10^{-3} wt. % using instantaneous γ -radiation from proton-induced nuclear reactions.

The available data on cross-sections of X-ray emission and γ -ray emission excitation processes, stopping powers of substances for protons and emission absorption in substances have been analyzed during the procedure development. It has been revealed that, despite of extensive experimental material [5, 6] and developed enough theoretical representations [7], there is a certain ambiguity in values of K-shell X-ray production cross-sections for elements with $Z > 70$ and proton energies of 3 MeV and higher. Therefore, the K-shell X-ray production cross-sections and intensity ratios for certain lines in a series for elements with atomic numbers in range 72–75 and proton energy 1–3 MeV have been measured at the first stage. The obtained experimental data have been used to develop a determination procedure of elemental content of tungsten-rhenium alloys.

The measurements of cross-sections, the procedure development and the analysis of objects were carried out using an "Elean" unit [8]. The unit is shown schematically in Fig. 1. The main unit assemblies are electrostatic charged particle accelerator, beam formation system, irradiation chamber with devices for target displacements and absorptive foil changes, the vacuum system, the detecting and spectrometric equipment.

An ESU-4.5 accelerator (Van de Graaff) provided a proton beam with energy from 400 keV up to 4.5 MeV at the energy resolution of 0.05 %. The beam current on a target in experiment was varied within limits of 100 to 300 nA, and current density, accordingly, within the range of $1 \cdot 10^3$ to $3 \cdot 10^3$ nA/cm².

The beam in the irradiation chamber was shaped by means of quadruple lens and system of diaphragms. To increase the beam homogeneity, it was defocused by lens, and to irradiate the target, the beam central part was used which was cut out by means of three diaphragms, the distance between the extreme ones being 130 cm. Two diaphragms nearest to the accelerator were shaped as tantalum foil disks with 3 mm interior aperture diameter. One of six dia-

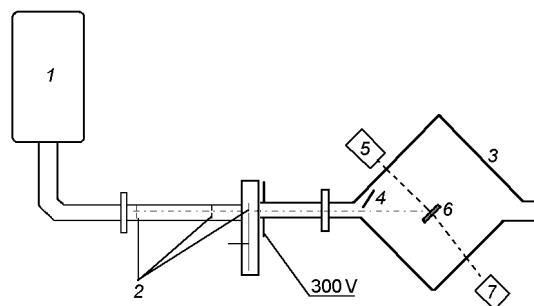


Fig. 1. "Elean" unit. 1, electrostatic accelerator; 2, beam shaping system; 3, irradiation chamber; 4, Si surface barrier detector; 5, Si(Li), GeHp detector; 6, target; 7, Ge(Li) detector.

phragms may be used as the last one, three from which made from carbon with orifice diameters of 1, 2 and 3 mm, and three are "combined", double-layer, consisting of tantalum and lead disks, with the same aperture diameters as the carbon ones. These diaphragms are interchangeable without vacuum deterioration. The use of double-layer diaphragms instead of carbon ones provides a background reduction in the X-ray channel by 30 %. A conductive cylinder under negative potential of 300 V located downstream the last diaphragm and electrically isolated therefrom was used to suppress secondary electrons arising in the beam formation system.

The irradiation chamber is a cylinder from antimagnetic iron of 310 mm in diameter and 100 mm height with covers at both butts. In the cylinder side surface, there are nipples for connection with vacuum system the chamber fixation on the table, pressure measurement as well as vacuum inputs for mechanisms of target displacement and X-ray filter change. The plane of cylinder base (the first cover) is located at angle 45° to direction of proton beam. It is provided with three inputs for connection of the chamber to ion guide at various orientations in the space, two windows for visual checking of irradiation and change of analyzed objects and absorbers, and a hole for installation of Si(Li) or GeHp detector. On the cover interior surface, mounted are the insulator setting the distance between the target and the Si(Li) detector, the X-ray collimator, and the disk with X-ray emission absorbers. A semiconductor Ge(Li) γ -emission detector is placed outside of the chamber, immediately behind the back cover.

Inside the chamber, the target device is installed. It contains a vertically movable frame where the horizontally movable cartridge for the targets is placed and two drive units providing horizontal and vertical displacement. 42 targets of 10 mm diameter can be fixed in the cartridge. The drives allow to place any of targets under the beam and to scan the target surface by a beam at an horizontal accuracy of 0.25 mm and vertical of 0.3 mm by independent displacements along mutually perpendicular directions.

The irradiated surface of a target, independently of its thickness, is placed in identical geometrical conditions: at angle 45° to bombarding beam axis and normal to the X-ray detector surface. The target surface is located in plane where the vertical and horizontal displacements are realized. Between Si(Li) detector and the target under irradiation, one of ten absorbing filters can be placed if necessary. The filters consisting of foils with known chemical compound and thickness are mounted on a rotating disk. The disk rotation mechanism is connected to a drive located on lateral surface of the chamber by means of worm gear. By choosing appropriate absorbers, it is possible to optimize the operating conditions of spectrometric equipment in the X-ray channel. A current integrator connected immediately to the chamber (that is electrically insulated from detecting system and ion guide) is used to measure the charge of protons accumulated on the target. The charge measurement error makes 1 % in current range of 1–500 nA. The chamber together with detecting system is located on a top plate of adjusting table. The table design allows to displace the plate with the devices located thereon in three mutually perpendicular directions within limits of 100 mm. The vacuum system is provides a vacuum in the chamber and is oil-free. It includes a silica gel pump, two coal ones and magneto-discharged NORD-250 pump and provides the residual pressure of 10^{-3} – 10^{-4} Pa. The detecting system includes three detecting blocks providing registration of characteristic X-rays, of charged particles elastic-scattered or arising in nuclear reactions, and gamma-quanta.

The Si(Li) X-ray detector is located at the angle 135° to the movement direction of incident particles at 70 mm distance from the target surface to attenuate the bremsstrahlung background. Between the detector and target, the X-ray emission col-

limator is located, that provides the effective detector area restriction to the central part making 50 % from the whole sensitive surface of the detector crystal, to eliminate the edge effects. The X-ray emission collimator includes two groups of diaphragms. Each group is an assembly of alternating two tantalum and two lead disks. The diaphragm nearest to the target is tantalum. The use of such a collimator has allowed to reduce considerably the total background of the X-ray channel in comparison with that observed with usual carbon diaphragms. No M and L lines of tantalum and lead have been revealed at control measuring of X-ray emission spectrum during 3600 s from zirconium target at proton energy 3 MeV and the beam current 50 nA. The elastic-scattered charged particles and those arising in nuclear reactions are registered by a Si surface barrier detector disposed at angle 170° to the beam axis, 70 mm from a target. The γ -radiation in the quanta energy range of 100 keV to 10 MeV is registered through the chamber back cover using a Ge(Li) detector placed outside the chamber at angle 55° to the beam direction, 75 mm from the target.

The K-shell X-ray production cross-sections of Hf, Ta, W, Re atoms was measured on thick targets following traditional technology. The 100 μm thick, 10 mm diameter disks of special purity Hf, Ta, W, Re foils were used as targets. To suppress the low-energy X-ray background and strong L-series radiation of the studied elements, a 60 μm thick tantalum foil absorber was placed in front of GeHp detector.

The accelerator was energy calibrated using the resonance at proton energy 991.88 keV from $^{27}\text{Al}(p,\gamma)^{28}\text{Si}$ reaction. The absolute efficiency of detecting system was determined using measurement of count intensities for standard radioactive sources located in the target position. ^{241}Am and ^{154}Eu sources were used for calibration. Experimental efficiency values were approximated by function of the type

$$\varepsilon = a \cdot E_x^b, \quad (1)$$

where ε is the detecting system efficiency; E_x , is the quantum energy; a , b , constants obtained by fitting of the experimental efficiency values using least square method. The fitting error did not exceed 3 %.

The X-ray emission spectra for all the elements were measured at proton energy of 1 to 3 MeV at 100 keV steps. When processing the spectra, the areas of $K_{\alpha 1}$, $K_{\alpha 2}$,

Table 1. Excitation cross-sections of K-series X-rays

| Proton energy, E_p (MeV) | Cross-section area, barn | | | |
|-------------------------------|--------------------------|---------|---------|---------|
| | Hf | Ta | W | Re |
| 1.0 | 4.69E-4 | 4.04E-4 | 3.48E-4 | 3.00E-4 |
| 1.1 | 7.01E-4 | 6.04E-4 | 5.20E-4 | 4.47E-4 |
| 1.2 | 1.01E-3 | 8.72E-4 | 7.54E-4 | 6.47E-4 |
| 1.3 | 1.42E-3 | 1.22E-3 | 1.05E-3 | 9.10E-4 |
| 1.4 | 1.94E-3 | 1.67E-3 | 1.44E-3 | 1.24E-3 |
| 1.5 | 2.59E-3 | 2.23E-3 | 1.93E-3 | 1.66E-3 |
| 1.6 | 3.41E-3 | 2.94E-3 | 2.53E-3 | 2.19E-3 |
| 1.7 | 4.40E-3 | 3.79E-3 | 3.27E-3 | 2.83E-3 |
| 1.8 | 5.61E-3 | 4.84E-3 | 4.15E-3 | 3.60E-3 |
| 1.9 | 7.05E-3 | 6.08E-3 | 5.24E-3 | 4.51E-3 |
| 2.0 | 8.77E-3 | 7.56E-3 | 6.53E-3 | 5.65E-3 |
| 2.1 | 1.08E-2 | 9.28E-3 | 8.02E-3 | 6.94E-3 |
| 2.2 | 1.31E-2 | 1.13E-2 | 9.76E-3 | 8.43E-3 |
| 2.3 | 1.59E-2 | 1.37E-2 | 1.18E-2 | 1.02E-2 |
| 2.4 | 1.90E-2 | 1.64E-2 | 1.41E-2 | 1.22E-2 |
| 2.5 | 2.26E-2 | 1.95E-2 | 1.68E-2 | 1.45E-2 |
| 2.6 | 2.67E-2 | 2.30E-2 | 1.98E-2 | 1.72E-2 |
| 2.7 | 3.13E-2 | 2.70E-2 | 2.33E-2 | 2.02E-2 |
| 2.8 | 3.67E-2 | 3.16E-2 | 2.72E-2 | 2.36E-2 |
| 2.9 | 4.26E-2 | 3.67E-2 | 3.16E-2 | 2.74E-2 |
| 3.0 | 4.92E-2 | 4.24E-2 | 3.65E-2 | 3.16E-2 |

$K_{\beta 1,3}$, $K_{\beta 2}$ peaks were determined. The calculated peak areas for corresponding energy lines, the detecting system efficiency, and the measured charge of the protons hitting the target were used to determine the X-ray emission yields taking into account the radiation absorption in the tantalum foil. The obtained yield values for each element were approximated by function of the type

$$Y = d \cdot (E_p)^f, \quad (2)$$

where Y is the yield of K-series X-rays; E_p , the proton energy; d and f , the constants determined for each element over the whole set of experimental points.

The formula [9] was used to determine the X-ray emission excitation cross-sections using the X-ray yields from thick targets:

$$\sigma(E_p) = \frac{4\pi}{\Omega \varepsilon n} \left(\frac{dY}{dE} S(E) + \mu Y \right)_{E=E_p}, \quad (3)$$

where $\sigma(E_p)$ is the K-shell X-ray production cross-section for protons of energy E_p ; Ω , the detector solid angle; ε , the X-ray emis-

sion registration efficiency of the detector; n , the density of atoms in the target material; Y , the X-ray emission yield, quanta per particle; dY/dE , the derivative of yield with respect to energy, determined by differentiation of expression (2); μ , the linear absorption coefficient of X-ray emission in the target material [10]; $S(E)$, stopping power of the target substance with respect to protons of energy E [11]. The K-shell X-ray production cross-sections calculated using the formula (3) are presented in Table 1.

The cross-section determination error was 6 to 12 %, depending on the proton energy. It was determined taking into account the following errors: statistical, 0.3 to 3 %; charge measurement, 1 %; absolute efficiency determination, <6 %; the dY/dE determination, <5 %; errors of proton stopping power tables, <5 %; and X-ray emission absorption coefficient, <5 %.

In Fig. 2, dependence of obtained experimental K-shell X-ray production cross-sections on proton energy is shown for all the elements. Comparison of the experimental

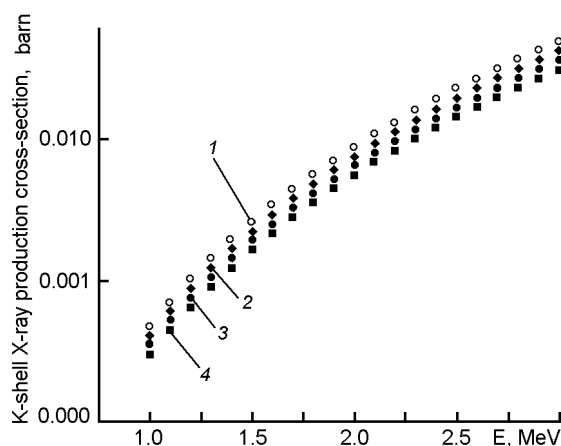


Fig. 2. K-series X-ray excitation cross-sections by protons for Hf(1), Ta(2), W(3), Re(4). (abscissa: Proton energy, MeV; ordinate: X-ray excitation cross-section, barn).

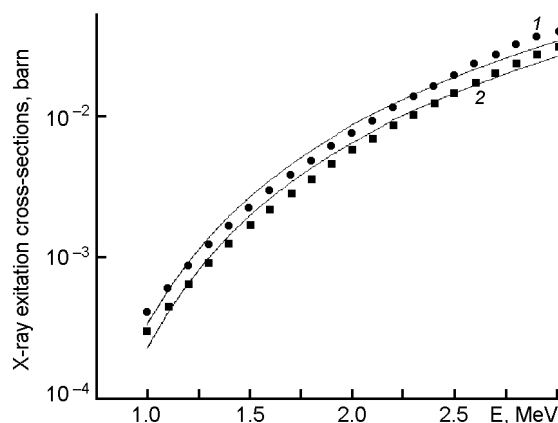


Fig. 3. Comparison of experimental cross-sections with those calculated using the formula from [5]: Ta(1), Re(2) (abscissa: Proton energy, MeV; ordinate: X-ray excitation cross-section, barn).

K-shell X-ray production cross-sections values from this work with those calculated from empirical formula proposed in [5] and being used widely in the analytical practice is shown in Fig. 3. Comparison of the experimental K-shell X-ray production cross-section values for tungsten from this work and results by other authors [12, 13] has shown a good agreement in the studied energy range; for other elements, experimental data are absent. The cross-sections calculated using empirical formula from [5] are agreed with experimental values within the experimental error, but as it is obvious from the curve run, at proton energies exceeding 2.5 MeV, the values calculated using the formula from [5] show a systematic underestimation with respect to experimental ones. This testifies to necessity to consider such circumstance when using this formula to estimate the K-shell X-ray production cross-sections at atomic numbers above 70 and high proton energies.

In Table 2, the intensity ratios of lines for K-series obtained in this work and calculated theoretically [14] are given. The intensity ratios have not found to differ essentially for various proton energy and have been averaged. As it is obvious from the Table, these quantities are close to theoretically predicted ones in most cases.

The K-shell X-ray production cross-sections and the intensity ratios for X-ray emission lines obtained in this work have been used to develop a determination procedure for heavy elements by PIXE using the K-series X-ray emission. As a rule, elements with atomic numbers above 50 are determined using the L-series radiation, because the yield of K-series X-ray emission at the same proton energy is 2–3 orders lower. However, in this case, the object under analysis contains elements with the close atomic numbers, and there are diffi-

Table 2. Line intensity ratios in the K-series.

| Element | $K_{\alpha_2}/K_{\alpha_1}$ | $K_{\beta_{1,3}}/K_{\alpha_1}$ | K_{β_2}/K_{α_1} | K_{β}/K_{α} | $K_{\beta_2}/K_{\beta_{1,3}}$ |
|---------|-----------------------------|--------------------------------|----------------------------|------------------------|-------------------------------|
| Hf | 0.589 ± 0.032 | 0.291 ± 0.016 | 0.076 ± 0.012 | 0.227 ± 0.013 | 0.249 ± 0.023 |
| | 0.572* | 0.312 | 0.070 | 0.253 | 0.225 |
| Ta | 0.592 ± 0.030 | 0.300 ± 0.014 | 0.078 ± 0.014 | 0.237 ± 0.014 | 0.253 ± 0.023 |
| | 0.574 | 0.313 | 0.071 | 0.255 | 0.227 |
| W | 0.599 ± 0.031 | 0.285 ± 0.015 | 0.071 ± 0.012 | 0.219 ± 0.017 | 0.256 ± 0.021 |
| | 0.576 | 0.315 | 0.072 | 0.257 | 0.228 |
| Re | 0.596 ± 0.030 | 0.271 ± 0.034 | 0.079 ± 0.013 | 0.221 ± 0.019 | 0.259 ± 0.023 |
| | 0.578 | 0.317 | 0.073 | 0.258 | 0.229 |

culties with separation of closely located peaks of L-series in X-ray spectrum. This problem does not exist when the K-series is used. Besides, effective thickness of analyzed layer is essentially increased, since the soft L-series radiation is essentially absorbed in the sample volume.

During measurement of K-shell X-ray production cross-sections, the conditions have been optimized for analysis of tungsten and rhenium alloys. It has been found that it is reasonable to carry out the analysis at the proton beam current of 100–200 nA and the energy 3.0 MeV. The analyzed layer depth at the used geometrical conditions and particle energy is about 20 μm . The absorbing foil were applied to suppress the low-energy background and intense L-series X-ray emission of tungsten and rhenium. The 20 and 40 μm thick iron foils, 20 μm thick tungsten, 100 and 160 μm thick aluminum and 60 μm thick tantalum ones were tried as absorbers. Acceptable level of count rate, shape of spectral lines and sufficient statistical error at the measurement time of 10^{-15} minutes have been obtained with tantalum foil as the absorber. The X-ray and low-energy (up to 200 keV) γ -radiation spectra were registered by semiconductor GeHp detector. A typical X-ray spectrum is shown in Fig. 4. Since the $K_{\alpha 1}$ -line of W and $K_{\alpha 2}$ -line of Re in the spectrum are superimposed, the X-ray emission $K_{\alpha 2}$ line (57.97 keV) was used to determine the W concentration while Re was determined using $K_{\alpha 1}$ -line (61.13 keV).

It is possible to determine the fluorine content simultaneously with tungsten and rhenium using PIGE at the proton energy 3 MeV. For this purpose, nuclear reaction $^{19}\text{F}(p,\alpha\gamma)^{16}\text{O}$ or $^{19}\text{F}(p,p'\gamma)^{19}\text{F}$ can be used. Each reaction provides some advantages and the use any of them depends on the requirements to the analysis.

The reaction $^{19}\text{F}(p,\alpha\gamma)^{16}\text{O}$ proceeds with formation of the intermediate nucleus $^{20}\text{Ne}^*$ which arises in the excited state. As a result of α -decay of the intermediate nucleus, a $^{16}\text{O}^*$ nucleus in the excited state is formed. Transition of this nucleus to the ground level is accompanied by emission of γ -quanta with energies 6.13, 6.92, and 7.12 MeV. The reaction cross-section within the proton energy range of 0.8 to 1.4 MeV has three narrow, intense resonances at 0.873, 1.347, and 1.374 MeV, and varies rather smoothly at proton energies exceed-

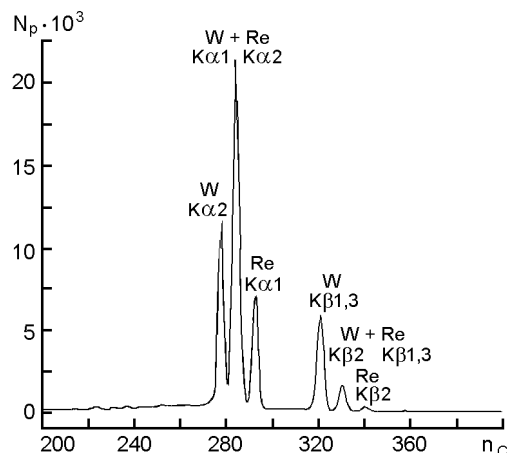


Fig. 4. K-series X-ray spectrum for a W-Re alloy. (abscissa: channel No; ordinate: count number).

ing 2.0 MeV [15]. Such character of cross-section dependence on energy allows to measure, if necessary, the fluorine concentration profile over the sample depth or to determine fluorine concentration in thin surface layers. So, when using protons with energy 873 keV, 80 % of γ -quanta generated in $^{19}\text{F}(p,\alpha\gamma)^{16}\text{O}$ reaction is emitted from 0.03 μm thick tungsten layer. Because of absence interfering lines of γ -radiation at the used proton energy, fluorine can be determined using that reaction at low concentrations (up to 10^{-5} wt. %) at a high accuracy.

The γ -quanta with 110, 197, and 1236 keV energy are originated in reaction $^{19}\text{F}(p,p'\gamma)^{19}\text{F}$. The presence of intense γ -radiation lines in the energy range up to 200 keV enables to register analytical lines of K-series X-ray of tungsten, rhenium and low-energy γ -lines of fluorine by GeHp detector in the same spectrum. This allows to use one spectrometer channel, thus simplifying the analytical data obtaining procedure and enhancing the fluorine determination accuracy at the analysis. The latter circumstance has defined the selection of γ -radiation lines with 110 and 197 keV energy from reaction $^{19}\text{F}(p,p'\gamma)^{19}\text{F}$ for determination of F. In Fig. 5, a γ -radiation spectrum of a typical tungsten-rhenium alloy sample is shown. Along with radiation lines of the main alloy components, lines of fluorine γ -radiation are seen therein. The 110 keV line has a higher intensity, but it interferes with the 111 keV line of tungsten from reaction $^{184}\text{W}(p,p'\gamma)^{184}\text{W}$. On the contrary, the lower intensity line at 197 keV in γ -radiation spectrum from tungsten-rhe-

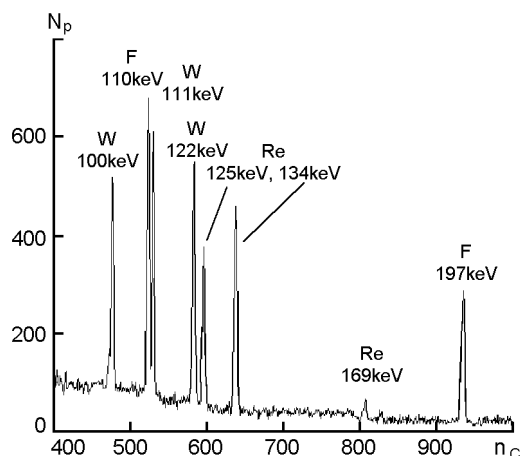


Fig. 5. γ -Radiation spectrum for a W-Re alloy. (abscissa: channel No; ordinate: count number).

niun matrix is in favorable conditions for determination, being on a smooth background without near peaks. Both lines can be used to determine as low fluorine concentrations as 10^{-4} wt. %.

If the element to be determined is distributed homogeneously in the sample, the yield of X- or γ -quanta emitted from a thick target per one incident proton with energy E_p is determined as

$$Y(E_h) = C\varepsilon \frac{\Omega}{4\pi} \int_0^{E_p} \frac{\sigma(E)\exp[-\mu x(E)]}{S(E)} dE, \quad (4)$$

where C is the atomic concentration of the element to be sought in the target substance; $x(E)$, thickness of the target layer where the element analytical emission is attenuated; $\sigma(E)$, K-shell X-ray production cross-section or cross-section of γ -quanta production by protons with energy E . Other symbols designate the same as in (3). Determination of a sample elemental composition with evaluation of integral (4) and solution of the equation for concentration now is used even more often in the analytical practice (the absolute method). However, there are a number of the circumstances allowing to simplify considerably the formula (4) at the determination of tungsten and rhenium in an alloy sample using K-series X-rays. In particular, the distinctions in absorption coefficients for K-series X-ray emission of rhenium and tungsten and stopping power of protons for matrices with boundary values of concentrations have been estimated

to be insignificant when 3.0 MeV protons are used. The account for these differences contributes less than 0.3 % to yields of X-ray emission. Because the fluorine γ -radiation is harder than X-ray emission, the distinction in absorption coefficients in this case is unessential at all. Thus, according to [16], the formula (4) may be rewritten in this case as

$$C = \frac{\nu Y S(E_{cp})}{\varepsilon Q E_p \sigma(E_p)} = K \frac{Y}{Q}, \quad (5)$$

where Q is the charge of protons stored at the target irradiation; ν , K constants, specific for each element. However, there are quantities $\sigma(E)$, $S(E)$, ε in the formula (5) for which it is necessary to use the reference or experimental values. Therefore, an error is contributed to the final result that is large enough and characteristic for those quantities. For the samples under study, that error was 8–20 % when concentrations were calculated using the formula (5). We have used the relative method proposed in [17] to improve the determination accuracy. The method is based on the statement that requirement of normalization $\sum_i C_i = 1$ is

satisfied at determination of all elements presented in the sample. Then the formula for evaluation of concentration looks like

$$C_i = \frac{Y_i}{n \frac{Y_i^{st} C_i^{st}}{\sum_{j=1}^n Y_j \frac{Y_j^{st} C_j^{st}}{Y_j^{st} C_i^{st}}}}, \quad (6)$$

where C_i is the i -th element concentration in the object being analyzed; Y_i , Y_j yields of X-ray emission or γ -radiation, respectively, for i -th and j -th elements from the object; similar symbols with upper index "st" mean the corresponding quantities for the reference sample. In such calculation of concentrations, the charge Q measurement error is eliminated also, since the yield ratios are used for calculations that depend only on statistical accuracy of the peak calculation. The final relative error of concentration calculations for determined elements using the above relative method amounted: for fluorine, 15–4 % at concentrations 0.0001–0.01 wt. %; for tungsten, 0.5–0.3 % at

concentrations 70–99.99 wt. %; for rhenium, 15–2 % at concentrations of 0.1–30 wt. %.

Thus, the IBA methods based on using of proton beams may be used successfully to determine the composition of tungsten-rhenium alloys or real pieces made of similar substances. The analytical procedure is ecologically safe and does not demand complex sample preparation. The obtained metrological performances of the analysis met the necessary normative requirements.

References

1. R.I.Jaffee, D.J.Maykuth, R.W.Dougllass, Rhenium and the Refractory Platinum-group Metals, Paper presented at the Aim Refractory Materials Symposium, Detroit (1960).
2. E.M.Savitskiy, M.A.Tylkina, K.B.Povarova, Rhenium Alloys, Nauka, Moscow (1965) [in Russian].
3. D.A.Robins, *J.Less-common Metals*, **1**, 396 (1959).
4. E.M.Savitskiy, K.B.Povarova, P.V.Makarov, Tungsten Metal Science, Metallurgiya Moscow (1978) [in Russian].
5. H.Paul, J.Muhr, *Phys. Reports*, **135**, 47 (1986).
6. L.Campbell, T.L.Hopman, J.A.Maxwell et al., *Nucl.Instr.Meth. in Phys.Res.*, **B170**, 193 (2000).
7. G.Lapicki, *J.Phys.Chem.Ref.Data*, **18**, 112 (1989).
8. A.N.Dedik, O.I.Ekhichev, V.V.Levenets et al., *Vopr.Atom.Nauki i Tech.Ser:Obshch. i Yad.Fiz.*, **2**, 48 (1981).
9. E.Merzbacher, H.W.Lewis, in: Encyclopedia of Physics, ed. by S.Flugge, Springer-Verlag, Berlin-Gottingen-Heidelberg, 1958, v.34, p.166.
10. B.V.Robouch, A.Cicerhia, *Comit.Naz.Ener.Nucl.*, **55**, 1 (1980).
11. J.F.Janni, *At.Data Nucl.Data Tables*, **27**, (1982).
12. M.Gogolowsky, M.Jaskola, J.Szerypo et al., *J.Phys.*, **B16**, 3571 (1983).
13. N.V.Castro Faria, F.L.Freire, E.C.Montenegro et al., *J.Phys.*, **B17**, 2307 (1984).
14. J.H.Scofield, *At.Data Nucl.Data Tables*, **14**, 121 (1974).
15. I.Goliceff, M.Loeyillet, Ch.Engelmann, *J.Rad.Chem.*, **12**, 233 (1972).
16. V.V.Levenets, A.P.Omelnyk, A.O.Shchur, *Vopr.Atom.Nauki i Tech.Ser:Vakuum, Sverchprovod., Chist.Metal.*, **6(14)**, 47 (2004).
17. USSR Author's Cert. No.1137889 (1985).

Використання методів PIXE і PIGE для дослідження сплавів на основі вольфраму і ренію, отриманих методом CVD

В.В. Левенець, А.О. Щур, О.П. Омельник, Б.М. Широков.

Представлено використання ядерно-фізичних методів на пучках протонів з реєстрацією рентгенівського випромінювання К-серії для визначення вольфраму та фтору і ренію у подвійних сплавах, отриманих за допомогою газофазного методу, і гама випромінювання для визначення домішок фтору.